3D Printed Hair Modeling from Strand-level Hairstyles

Han Chen
Shandong University
Qingdao, China

Minghai Chen
Shandong University
Qingdao, China

Lin Lu
Shandong University
Qingdao, China
llu@sdu.edu.cn

Abstract

Recent advances in the design and fabrication of personalized figurines have made the creation of high-quality figurines possible for ordinary users with the facilities of 3D printing techniques. The hair plays an important role in gaining the realism of the figurines. Existing hair reconstruction methods suffer from the high demand for acquisition equipment, or the result is approximated very coarsely. Instead of creating hairs for figurines by scanning devices, we present a novel surface reconstruction method to generate a 3D printable hair model with geometric features from a strand-level hairstyle, thus converting the exiting digital hair database to a 3D printable database. Given a strand-level hair model, we filter the strands via bundle clustering, retain the main features, and reconstruct hair strands in two stages. First, our algorithm is the key to extracting the hair contour surface according to the structure of strands and calculating the normal for each vertex. Next, a close, manifold triangle mesh with geometric details and an embedded direction field is achieved with the Poisson surface reconstruction. We obtain closed-manifold hairstyles without user interactions, benefiting personalized figurine fabrication. We verify the feasibility of our method by exhibiting a wide range of examples.

Keywords: Hair Modeling, Strand-level Hairstyles, 3D Printing

1. Introduction

The hair plays an important role in creating a digital avatar or fabricating a personal portrait in the computer graphics community. The generation of 3D hair models is in high demand; however, it requires significant technical and artistic expertise and manual labor to model a hairstyle due to various hairstyles and different hair structures. The hair data captured directly by the current technique is usually inadequate for figurines fabrication.

Physical reproduction in general, particularly humans, has become a hot topic in academia and industry. [15] proposed a pipeline that reconstructs a 3D printable portrait using a single Kinect sensor which is quite user-friendly, but the detailed geometry structure of the hair is lost. Although the printable portrait reconstruction in [9] is high-end and able to preserve the essential look of the real hair, however, the method could only be operated in a well-controlled studio environment, and the hairstyle is limited to the subject. The underlying pipeline of these systems is similar, involving 3D scanning and fabrication-aware model reconstruction for a specific user. Therefore, these reconstruction systems have similar limitations, and in particular, producing a variety of optional hairstyles in a short time is impossible. Progress in data-driven and neural networks has contributed a lot to the development of digital hairstyle modeling. In the digital hair modeling field, the high-fidelity modeling of strand-level hair is possible within a few minutes from a single image [20, 12, 6], contributing many kinds of strand-level hair databases. A 3D printable model has constraints on geometries, as manifold and watertight. Nevertheless, these digital hairstyles, represented by strands composed of vertices, do not meet printing constraints and cannot be directly applied to manufacturing. We hope to apply these digital hairstyles to portrait fabrication.

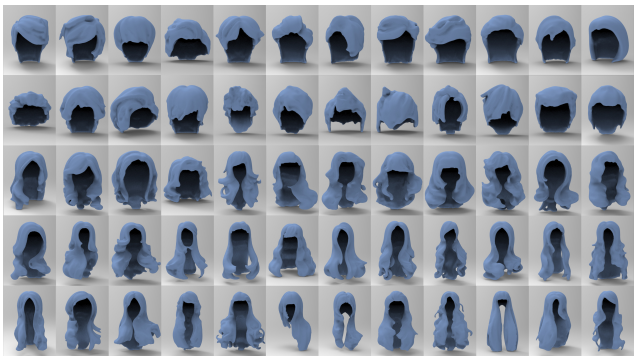

Figure 1: Partial of the hair model data-set reconstructed by our method.

The digital hairstyle can hardly be fabricated directly. Attempts have been made to fabricate hair-like structures

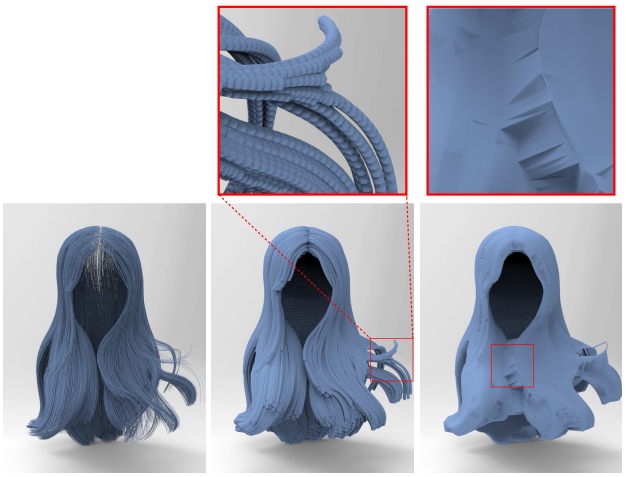

(a) (b) (c)

Figure 2: Given an input strand-level hairstyle (a), thickening each strand to a valid volume causes large data size, leading to unstable slicing and complex support structures in fabrication (b); traditional surface reconstruction like [26] may cause mistakes around the border area (c).

like strands, fibers, or tree branches, etc., based on different 3D printing techniques, via programming the nozzle movement [14], manipulating with hair structures and high-resolution stereolithography [19], or adaptive geometry reduction and optimizations [2]. However, the printable geometry is limited since these filaments collapse under gravity before hardening and cannot be posed arbitrarily without support. The hairstyle strands are too fragile to afford support structures. Robotic 3D printing may help to reduce support structures, but collisions between the model and printing platform become another challenging problem. Thickening the strands to meet fabrication constraints would make the file size too large because the number of vertices in the digital hair is huge (about 1 million). When a strand is thickened into a geometric shape represented by a series of cylinders as shown in Figure 2b, the data size of the model becomes enormous, and the effect of traditional simplified methods on simple cylinders are limited, making the whole model infeasible for processing in commercial 3D-print software. Rare techniques focus on reconstructing fine appearance, watertight mesh from strand-level hair that satisfies fabrication constraints. Traditional methods [1, 24, 26] can extract the boundary of points set. They suffer from poor reconstruction quality or do not conform to the structural characteristics of the hairstyle because the results of these methods are determined by the vertices density rather than structural characteristics. [30, 27] utilize methods to generate triangle meshes from strand-level hair by a signed distance field. They focus on the rough shape of strands, as shown in Figure 2c, therefore, not closely representing the growing trends of the original hair. This results in the lack of details in the hairstyles for manufacturing.

This work aims to fill the gap in reconstructing 3D printable models according to the structure of strands from strand-level hair and provides a 3D printable hairstyles database. Figure 1 shows part of the database generated by our method. In practice, high-resolution strands are generally too expensive for hairstyle presentations, while our manifold models are more practical. Moreover, many works such as [27, 21] need a close hair model with a direction field as ground truth for training. Our generated hair model contains a corresponding direction field as well.

We propose a two-stage reconstruction framework to accomplish this goal without any user interaction. Our method starts by filtering the strands of the input hair and retaining the primary growing trend on the surface. In the next step, a coarse-level hairstyle is reconstructed so that the normal of vertices is obtained and contour points are extracted by our algorithm. In the second stage, we reconstruct the fine-level model for this hairstyle based on implicit function from the contour points of the coarse-level model. Finally, we remesh the model to make the density controllable result for fabrication.

The main contributions of our work are as follows:

- A novel computational framework that reconstructs 3D printable hairstyles with geometric details from strand-level hairs.
- A reconstruction algorithm customized for hair strands that identifies the surface strand and preserves the hair trend.
- A 3D printable hairstyle database for figurine fabrication, and the correspondence between the strand-level hairstyle and its manifold counterpart.

2. Related Work

The generation of the 3D hair model is an extensively studied topic since it is one of the most time-consuming and the most challenging task in the human reconstruction field. Work related to ours includes hair strand modeling, hair reconstruction, and personalized figurines.

Hair Strands Modeling. It is pivotal for digital human reconstruction to do well in hair modeling. In the rendering level, modeling hair as the strands or wisps is a general and effective method studied well in the community. Strands type means high resolution and a large amount of data. Several approaches have recently been proposed for image-based hair modeling on the rendering level, which take images as input and then model the strands according to the hair features in those images. [12] proposes a method

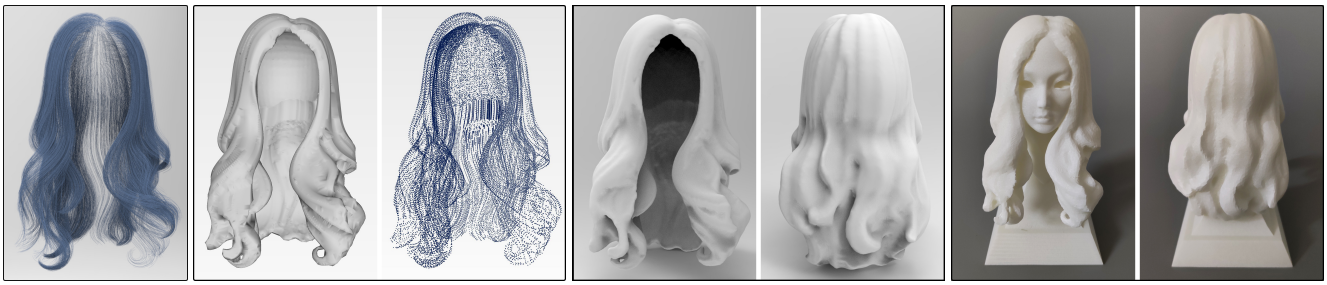

(a) Input (b) Coarse-level Reconstruction (c) Fine-level Reconstruction (d) 3D Printed Results

Figure 3: Pipeline overview. Our approach starts with an input hairstyle in strands (a), following with a coarse-to-fine reconstruction (b-c), and obtains the 2D manifold hair model that can be 3D printed (d).

based on a database to model the hair from a single-view photograph with some strokes from users. [27] introduces a data-driven approach to model a hairstyle from four-view images with some user interaction. [16] proposes an automatic method for modeling a personalized hairstyle from a short video.

Considerable progress has been made to deep learning for strand hair modeling. A fully automatic hair modeling pipeline from a single view has been introduced by [6], which estimates the hair region and growing direction using a deep neural network. [21] takes a single image as input, using a neural network for their training and inference algorithms to model the hairstyle with a similar structure as the image. [29] introduces a deep-learning-based method to generate full 3D hair geometry from an unconstrained image, with real-time performance. [22] proposes a deep-learning-based tool for interactive modeling of 3D hair from 2D sketches, which takes the time and effort of users.

These methods reconstruct hair as strands or wisps for rendering that do not meet the 3D printing constraints of a manifold surface, despite the nice appearances. Our method tackles the challenge of converting strand-level hair to printable hairstyle, reserving the strand structure and regards the strand-level hair as input to develop a closed mesh model for 3D printing.

Head Reconstruction. Human reconstruction is always a hot and classical research issue in the community, where researchers spend substantial effort in head reconstruction. [7] presents a single-view hair modeling for the application of image manipulation, whose primary goal is different from ours. High-quality hair relievos are obtained from a single portrait photo based on shape from shading (SFS) [5], which also represents fine details of the hairstyle. However, a high-contrast image as input is required to this method significantly since the SFS algorithm reconstructs objects by the lights-and-shadows information. What's more, one of the limitations of the SFS method is their output cannot exhibit the occupancy view of the hair, so it does not apply to our subject. [18] allows using volume shape prior to reconstructing the geometric structure of the human head in multiple views from structure-from-motion dense stereo matching. [4] has shown that a complete 3D head model with rough but unstable hair can be reconstructed from a set of captured images, and the depth of the hair can be estimated from each image and then merged together. [17] explores how to reconstruct a personal morphable head model from photos on the Internet. [8] reconstructs the human hair to a manifold surface based on structured light (SL) scanning system from multiple views. However, this method is not robust enough. Specifically, a specific hardware environment or a neat, locally consistent, and distinct subject's hairstyle can influence the result greatly due to the weak photonasty of the cluttered and dark hairlines. When the surface of the hair region is too distorted to recognize, the entire hairstyle and the local details are also inaccurate.

These methods focus on reconstructing the facial feature of the user. On the contrary, our approach intends to reconstruct a wide range of optional hairstyles from a strand-level hair database.

Personalized Figurines. Figurines design and creation is one of the most traditional and classical art forms in the world and people always tend to obtain a personalized figurine as artwork or souvenir. With the rapid development of 3D printing, several methods are employed to capture 3D printable human models. [15] develops an automatic pipeline that allows ordinary users to capture complete and fully textured 3D portrait models. A semi-automated system for fabricating figurines with personalized faces is presented by [25]. [23] describes a cost-effective approach to fabricate 3D miniatures of persons using a Kinect sensor and a 3D color printer, with detailed synthesis and small holes filling. All these works reconstruct portrait models or at least hairstyle models in low-resolution, and the results have a low level of geometric details. [9] captures personalized hairstyles for accurately physical reproduction. The physical results are highly detailed and fidelity; however, the costs are high. The system consists of 40 SLR cameras to capture the subject and reconstruct the original model;

meanwhile, a subset of eight views covering the hair volume from the front, back, and sides is selected. Problems may occur when the environment changes as the lighting directly influences the texture. [11] proposes a feasible solution for texturing 3D models of people using a low-cost RGB-D sensor. Despite a similar low cost and lightweight goal, this work aims at model coloring, which differs from our emphasis on a geometric shape.

3. Overview

We use the strand-level hair database from [12] as the input with 343 different hairstyles. Each hairstyle consists of about 10k hair strands. Our solution is motivated by QuickBundles (QB) clustering algorithm [10] for interpreting large numbers of streamlines. The pipeline of our two-stage algorithm for a 3D printable hair reconstruction from strand-level hairstyles is shown in Figure 3.

First, we reconstruct a coarse-level model from the input and extract the contour points of hair. Using a strands-filtering method for the hairstyle based on the QB algorithm, we filter sparse, inconsistent strands and keep the fidelity of input strands. Then, we repeat the reconstruction for a hair to obtain the contour points, extract the correct vertices representing the surface in a more-to-less fashion by our algorithm and calculate normal for each point.

We compensate the offset of vertices and reconstruct the fine-level model from the contour points with normals by screened Poisson surface reconstruction in the second stage. We also remesh the triangles with different densities and obtain a closed 2D manifold surface for 3D printing.

4. Technical Details

Our goal is to reconstruct the strand-level hair according to the structure of strands as shown in Figure 4. Details of the method are described in this section.

4.1. Coarse-level Reconstruction

Strands filtering. Though the scattered and uneven density distribution of strands over whole space makes hairstyles for digital avatars more real during rendering, they cause trouble to the surface identification for the fabrication. For strand-level hairs, the distribution of vertices is too varied to apply a uniform method. To obtain a clean reconstruction result, we classify and filter the useless strands by clustering over strands inspired by the QB method proposed in [10]. QB algorithm is very efficient and can reduce strands representation to an accessible structure in a time that is linear. Specifically, we cluster strands based on Euclidean distances bottom-up hierarchically. Given the input stand-level hairstyle I_0, we uniformly pick K points of a strand as the feature points to construct $K \times 3$ matrix F_i that represents the i-th strand. Then, we cluster F_i and record the number of strands of each cluster as W. Besides, we set the

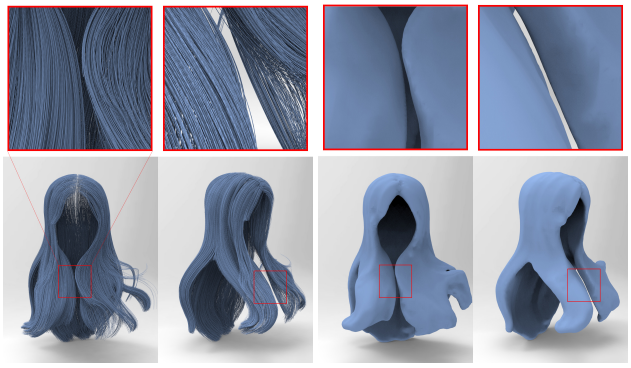

(a) (b)

Figure 4: (a) The input hairstyle (identical to Figure 2) has some strands very close in red box. (b) Our reconstructed result conforms to the strand structure.

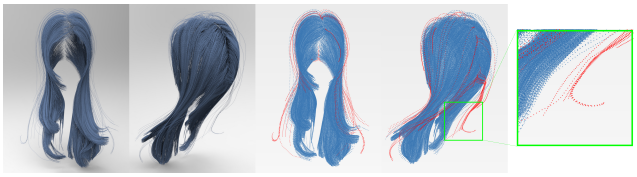

Figure 5: Strands filtering. The sparse strands near the surface are identified. Left two: a hairstyle in two views; right three: filtered strands are labelled in red and zoomed region is shown in green box.

cutoff number of clusters C. In the presented results, we use $K = 5$ and $C = 400$, which give a good trade-off between clustered quality and memory size reduction, for input hairstyles with around 10k strands.

We filter the sparse strands that may affect the reconstructed manifold structure. Heuristically, if a cluster with the number of strands is less than a threshold, it can be regarded as negligible in contributing to the manifold hairstyle. In practice,

$$I_0 \leftarrow \{c \mid W_c > \sigma N/C\}, \tag{1}$$

where W_c is the number of strands in the cluster c, N denotes the total number of strands, σ is set to 0.2. In this way, each strand is identified, we remove the clusters that do not satisfy the constraint. Figure 5 shows an example of strands filtering.

Contour points extraction. The hair strands are unsuitable for the reconstructions based on implicit function because those methods need accurate contour points with normal as input, which is usually obtained by scanning or modeling. Our goal is to extract the accurate contour points from strands. While the methods [1, 24, 26] can extract the boundary of points set, they suffer from the reconstruction quality and do not conform to the structural character-

istics of the hairstyle because the reconstructed surface of these methods is determined by vertex density rather than structural characteristics, as shown in Figure 4a. However, the true surface of the hair is not entirely determined by the density, the structure of strands also plays an important role.

Our contour points extraction algorithm repeats the reconstruction for a hair to obtain the contour points and extract the correct vertices in a more-to-less fashion. We first calibrate the position of the hairstyle I_0, with the top facing the positive y-axis and the front facing the positive z-axis. Second, based on the common features of strands distribution, we project the hairstyles in the three-dimensional space to the corresponding xz plane to get I_1 and xy plane to get I_2. After that, we cluster the three stands sets $\{I_i\}_{i=0}^{2}$ using the QB algorithm and get clusters c_i, respectively. Suppose that C_i is the cutoff clustering number for I_i, then C_0 is usually in [10, 20], and C_1 and C_2 is in the range [4, 10]. For each cluster c_{ij}, we denote its corresponding 3D point set in the original hair as P_{ij}. Then we reconstruct the contour points for each P_{ij} based on the alpha shape algorithm [26]. With the reconstructed mesh model, we calculate the face normal by the cross product of two adjacent edges of a triangle and process the adjacent meshes by growing to ensure the consistency of all face normals. The vertices normal is obtained by average the connected face normal with the weight of face area. Therefore, we obtain three sets of hairstyle contour points B_i containing the internal boundary points of the clusters and the corresponding normals. Finally, we obtain the intersection of three sets of hairstyle contour points B_i to remove the internal points and extract common contour points, which are the outer contour points $\mathcal{P}$ of the corresponding hairstyle. In the clustering, the contour points generated of three dimensions have the same outer contour, and the internal contour points of different dimensions are different. Because the clusters generated by clustering are different, the internal contour points will be removed in the logical operation. We obtain the outer contour points conforming to the structure of the strands. Refer to Algorithm 1 for details. An example of the extraction result is shown in Figure 3b.

4.2. Fine-level Reconstruction

All the hair strands are growing from the scalp, making the recognition of inner and outer layers around hairline regions difficult, as the distance between inner and outer points around hairline regions is too close. Although the quality of the implicit surface reconstruction method is better, it may cause vertices shifting, which may produce holes in the hairline regions. We apply a gradient displacement along the normal for each vertex to compensate for the offset and reduce its effect on the other regions. The gradient displacement function is

$$\acute{v(i)} = v(i) + \beta \times (1 - dis(i))^2 \times normal(i), \quad (2)$$

Algorithm 1: Coarse-level reconstruction

Input: A strand-level hair I_0
Output: Contour points $\mathcal{P}$

StrandsFiltering (I_0);
Calibrate (I_0);
$I_1 \longleftarrow$ *ProjectOntoXZPlane*(I_0);
$I_2 \longleftarrow$ *ProjectOntoXYPlane*(I_0);
for $i = 0 \rightarrow 2$ **do**
  $c_i \longleftarrow$ *QuickBundles*(I_i, C_i);
  for $j = 1 \rightarrow C_i$ **do**
    $P_{ij} \longleftarrow$ *Get3DPoints*(c_{ij});
    $b_{ij} \longleftarrow$ *AlphaShape*(P_{ij});
  $B_i = \sum_{k=1}^{C_i} b_{ik}$;
$\mathcal{P} = B_0 \cap B_1 \cap B_2$;

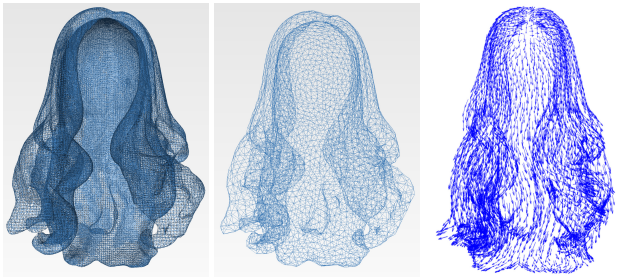

(a) (b) (c)

Figure 6: Remeshing result. The mesh reconstructed by SPSR (a), the model remeshed by isotropic explicit remeshing (b), the remeshed model embedded with the direction field (c).

where $\acute{v(i)}$ denotes point $v(i)$ after displacement, $dis(i)$ is the closest distance from $v(i)$ to the scalp. β is a weight of displacement affecting the result of overall displacement. In our work, β set to 1/10 of the longitudinal length of the scalp. This gradient displacement is small that has little impact on the overall appearance and structure of the hairstyle but is sufficient to distinguish the inner and outer points around hairline regions clearly. Even for some hairstyles such as buns ponytails, where the hair rises the scalp, the displacement also will not destroy the structure in the over-scalp region.

Next, we reconstruct triangle meshes over it using screened Poisson surface reconstruction [13], which achieves a high accuracy when there is no noise in the input. This reconstructed surface that restores the surface strand's growing trend is highly similar to the input hair model in overall shape.

Then we remesh the model by using the method of isotropic explicit remeshing [3], which lets the user freely choose the density of the mesh as shown in Figure 6.

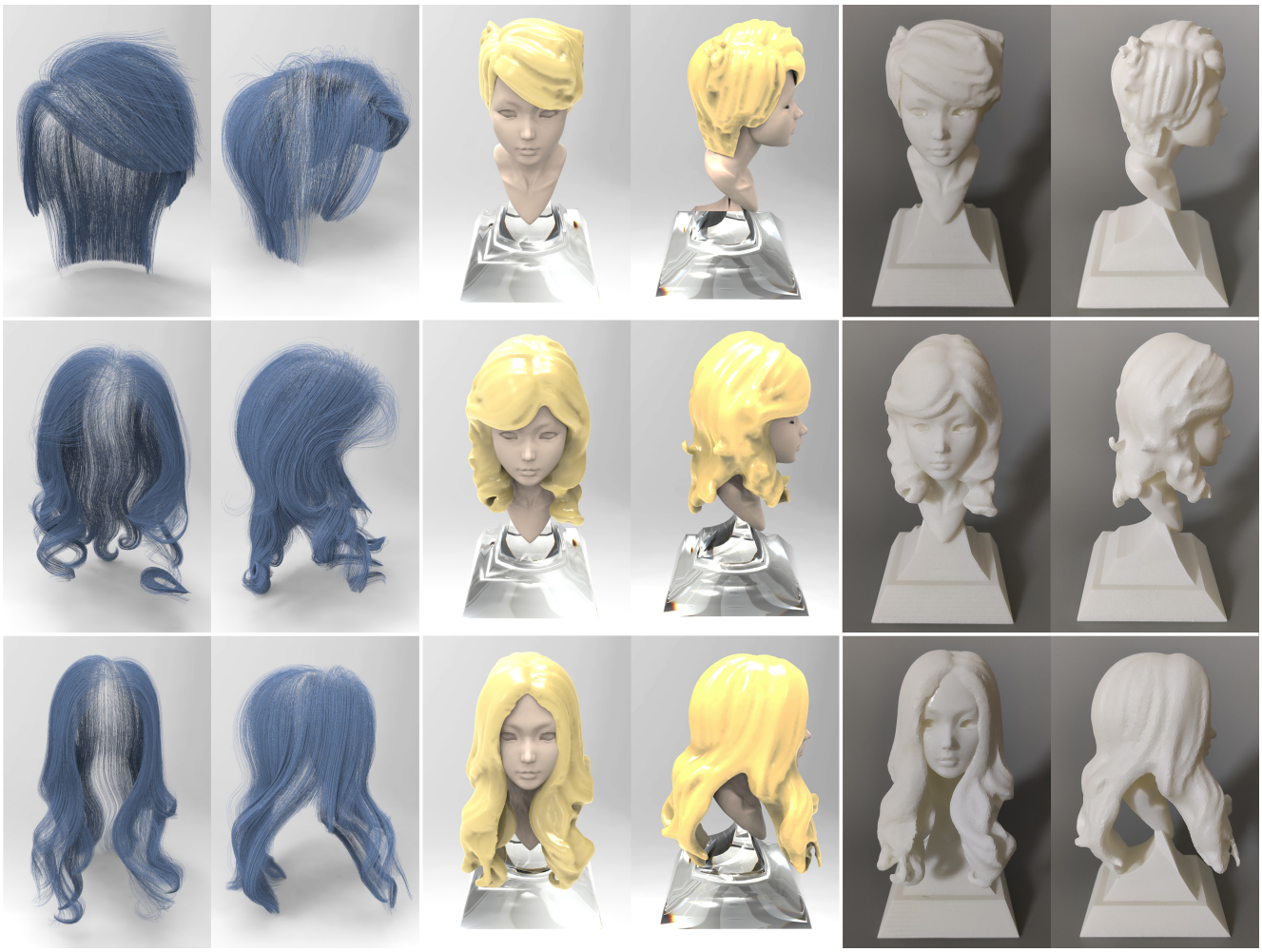

Figure 7: Reconstructed and 3D printed results from strand-level hairstyles. From left to right: input strands in two views, reconstruction results, and 3D printed results.

The results with high-density meshes are suitable to fabricate hairstyles for user or cartoon characters. The result, which represents the hairstyle's rough contour with a smaller amount of data, can be used for faster retrieving and geometry processing.

5. Results

Performance. All experiments are performed on a computer with an Intel i7-9700 CPU and 32GB of memory. Most input strand-level hair models consist of millions of vertices. The total processing time using our unoptimized pipeline is about 50 seconds. In general, for adequate representation of the features of the hairstyle, the suitable number of facets of a hairstyle is between 20k and 500k.

Fabrication. Physical printouts are fabricated using a Stereolithography (SLA) printer RSPro 600, with the accuracy ±0.1 mm. The height of each sculpture is approximately 20cm, the length and width are about 15cm. It takes about 10 hours to fabricate a portrait model solely; however, in practice, multiple models are packed together in the build volume to save the printing time. For example, the build volume of RSPro 600 is 600*600*400mm, which allows 15 sculptures packed together for fabrication; then the total time is around 27 hours. We reconstruct and fabricated a variety of hairstyles, including curly/short/long ones, as shown in Figure 7 and 8. For short or fluffy cases, our approach can also handle them and produce reasonable physical results. Note that support structures might be required for fabrication. Since the models are one piece closed mesh, the support structures are easily constructed and removed, and thus do not effect the model quality.

Database. A printable hairstyle database with 343 different hairstyles is generated by our method from a strand-level hair database [12]. Figure 1 shows partial results of the printable hairstyle database. Each model is a manifold wa-

Figure 8: Our hair modeling results for some special hairstyles, with short or chaotic strands. From left to right: input strands in two views, reconstruction results, and 3D printed results.

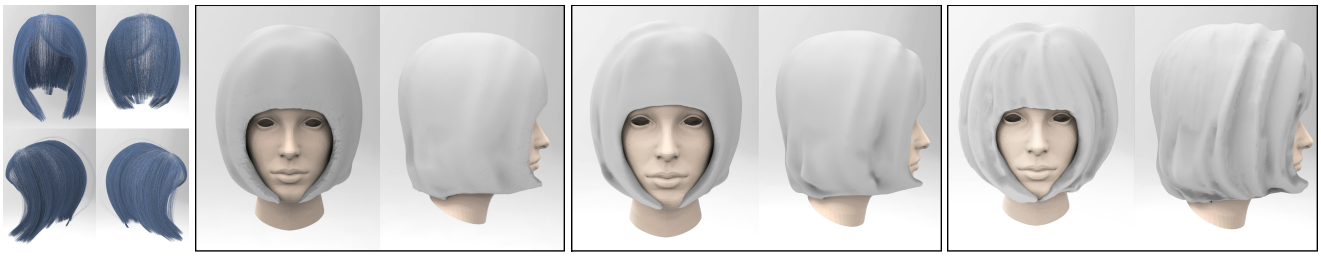

(a) Input (b) Voxelization and filter method (c) A signed distance field method (d) Our result

Figure 9: Comparison. From left to right, input hair strands (a), result reconstructed by voxelization and filter method (b), (c) is constructed using a signed distance field obtained by volumetric points samples, our result (d).

tertight triangular mesh that can be fabricated. Moreover, a direction field embedded into each hairstyle can extend the application scenarios of this database. To extract the underlying direction information of original strand-level hairs, we process the strand one by one and get the direction for each vertex following the sequence of vertices in each strand. For the final model, we search the nearest point of the input strand-level hair for each point of the model and thus update the direction field. The database is fully available online[1].

Comparisons. Traditional methods that can be applied directly to point clouds are not suitable for reconstructing strand-level hairstyles because the results of these methods are determined by the vertices density rather than structural

[1] https://github.com/lulinlinda/3D-Printed-Hair-Modeling-from-Strand-level-Hairstyles/releases

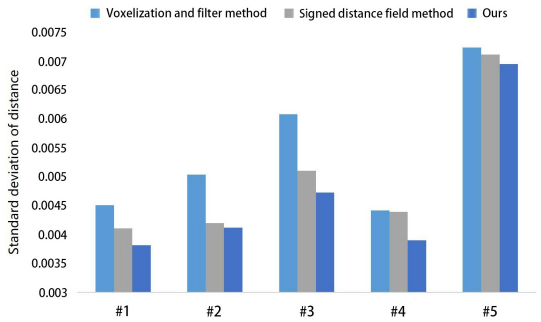

Figure 10: Evaluation of fidelity for reconstructed result by standard deviation of distance between input and result. We evaluate the voxelization and filter method (Figure 9b), the signed distance field method (Figure 9c), our proposed method by randomly picking 5 different hairstyles.

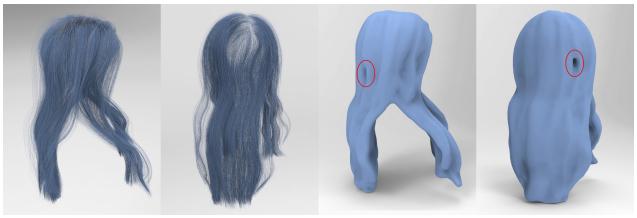

Figure 11: A failure case. Our method cannot faithfully handle hairstyles when the strands near the surface are very varied. Left two: input strands; right two: reconstructed result with an unnatural pitting on the back region. The main reason is that the surface points of these areas are not correctly identified.

characteristics as shown in Figure 2, and the implicit surface reconstruction method cannot be applied directly to the hair.

There are few methods to reconstruct strand-level hairstyle properly. To verify the effectiveness of our reconstruction method, we compare our method to several traditional reconstruction approaches. To ensure the fairness of the comparison, we replace the input of other methods with the same input as ours.

In Figure 9, we compare our method with the preprocessing step from [27], which uses signed distance field (SDF) [28] to convert strand data to voxels and then applies a blurring filter on the vertices of SDF. In comparison, this method gains a similar and smooth shape, but the geometric features of the surface are severely lost. In our approach, the details and growing trends of the strand make the hairstyle more natural and vivid for portrait fabrication.

Besides, we compare our method with the widely used method from [30]. This surface can be constructed using a signed distance field obtained by volumetric points samples. Visually speaking, this method can partially retain the geometric features of the hairstyle under the premise of generating a smooth surface. Although [30] reconstructs a smooth and manifold result. Compared with these methods, the details and growing trends of the strand make the hairstyle more natural and vivid for portrait fabrication by our method.

Evaluation. As shown in Figure 12, hairstyles represent the features of the input. We use the standard deviation of the distance to evaluate the fidelity of the reconstructed result. The output meshes are used as references. The evaluation index is obtained by calculating the standard deviation of the distance between each input vertex and the output surface. In general, the better the fidelity, the smaller the standard deviation of the distance.

We evaluate our method, a voxelization and filter method as Figure 9b and a signed distance field as Figure 9c to prove that our results are more consistent with the main contour of the original data. As shown in Figure 10, we randomly selected five hairstyles for comparison. The standard deviation of the distance is influenced by the thickness of the hair and the consistency of hair trend, and increases as the hair are thicker.

6. Conclusions

We have presented a surface reconstruction method for strand-level hairstyles that does not need any user interaction. We also provide a printable hairstyles database and an embedded direction field. High-fidelity reconstruction is made possible after the core step, including strand filtering and contour points extraction from strands by ours. A plausible hairstyle can be reconstructed from any available strand-level hair database. Our method has significant advantages compared with traditional reconstruction methods. It balances the compromise between the mesh quality and fidelity to input strands as we accurately extract the filtered surface and reproduce the growing trend of hairs on the reconstructed surface.

Our 3D hair reconstruction approach can be widely applied in portrait fabrication for various hairstyles from all the state-of-the-art strand-level hair databases. Besides, our method can be used for portrait fabrication, real-time rendering as the density of mesh is controllable and can also be used for neural network training [21]. While we focus on reconstructing 3D hairstyles, this method may be useful for a broad range of non-trivial shapes based on strands, such as furry animals and clothes.

Limitations and future work. Figure 11 shows a failure case, which reveals one limitation of our method. It is hard to distinguish the inside and outside the boundary when the density of strands is too varied, and some ”sparse” strands are not easily distinguishable in extreme hairstyles. We counted the failure case for each hairstyle to evaluate the robustness of our hair reconstruction method. The average successful reconstruction rate from the input is 98.6%. Moreover, it would be interesting to adaptively define the

Figure 12: Our hair modeling results of 5 different hairstyles. From left to right: input strands in four views, our modeling results in corresponding four views, and the results in a far oblique side view.

strand filtering strategy for different hairstyles rather than apply the same parameter to control the filtering method for all kinds of hairstyles. Finally, we are working on taking advantage of the manifold hairstyles to add more detailed textures to the 3D printed hair, with the hair image or other knowledge as the input.

Acknowledgement

We thank all the anonymous reviewers for their constructive suggestions. This work is supported by grants from NSFC (61972232) and the Special Project of Science and Technology Innovation Base of Key Laboratory of Shandong Province for Software Engineering (11480004042015).

References

[1] F. Bernardini, J. Mittleman, H. Rushmeier, C. Silva, and G. Taubin. The ball-pivoting algorithm for surface reconstruction. *IEEE Transactions on Visualization and Computer Graphics*, 5(4):349–359, oct 1999. 2, 4

[2] Z. Bo, L. Lu, A. Sharf, Y. Xia, O. Deussen, and B. Chen. Printable 3d trees. *Computer Graphics Forum*, 36(7):29–40, oct 2017. 2

[3] M. Botsch and L. Kobbelt. A remeshing approach to multiresolution modeling. In *Proceedings of the 2004 Eurographics/ACM SIGGRAPH symposium on Geometry processing - SGP '04*. ACM Press, 2004. 5

[4] C. Cao, H. Wu, Y. Weng, T. Shao, and K. Zhou. Real-time facial animation with image-based dynamic avatars. *ACM Transactions on Graphics*, 35(4):1–12, jul 2016. 3

[5] M. Chai, L. Luo, K. Sunkavalli, N. Carr, S. Hadap, and K. Zhou. High-quality hair modeling from a single portrait photo. *ACM Transactions on Graphics*, 34(6):1–10, nov 2015. 3

[6] M. Chai, T. Shao, H. Wu, Y. Weng, and K. Zhou. Autohair: Fully automatic hair modeling from a single image. *ACM Transactions on Graphics*, 35(4):1–12, jul 2016. 1, 3

[7] M. Chai, L. Wang, Y. Weng, Y. Yu, B. Guo, and K. Zhou. Single-view hair modeling for portrait manipulation. *ACM Transactions on Graphics*, 31(4):1–8, aug 2012. 3

[8] Y. Chen, Z. Song, S. Lin, R. R. Martin, and Z.-Q. Cheng. Capture of hair geometry using white structured light. *Computer-Aided Design*, 96:31–41, mar 2018. 3

[9] J. I. Echevarria, D. Bradley, D. Gutierrez, and T. Beeler. Capturing and stylizing hair for 3d fabrication. *ACM Transactions on Graphics*, 33(4):1–11, jul 2014. 1, 3

[10] E. Garyfallidis, M. Brett, M. M. Correia, G. B. Williams, and I. Nimmo-Smith. QuickBundles, a method for tractography simplification. *Frontiers in Neuroscience*, 6, 2012. 4

[11] C. Heindl, S. C. Akkaladevi, and H. Bauer. Capturing photorealistic and printable 3d models using low-cost hardware. In *Advances in Visual Computing*, pages 507–518. Springer International Publishing, 2016. 4

[12] L. Hu, C. Ma, L. Luo, and H. Li. Single-view hair modeling using a hairstyle database. *ACM Transactions on Graphics*, 34(4):1–9, jul 2015. 1, 2, 4, 6

[13] M. Kazhdan and H. Hoppe. Screened poisson surface reconstruction. *ACM Transactions on Graphics*, 32(3):1–13, jun 2013. 5

[14] G. Laput, X. A. Chen, and C. Harrison. 3d printed hair: Fused deposition modeling of soft strands, fibers, and bristles. In *Proceedings of the 28th Annual ACM Symposium on User Interface Software & Technology*. ACM, nov 2015. 2

[15] H. Li, E. Vouga, A. Gudym, L. Luo, J. T. Barron, and G. Gusev. 3d self-portraits. *ACM Transactions on Graphics*, 32(6):1–9, nov 2013. 1, 3

[16] S. Liang, X. Huang, X. Meng, K. Chen, L. G. Shapiro, and I. Kemelmacher-Shlizerman. Video to fully automatic 3d hair model. *ACM Transactions on Graphics*, 37(6):1–14, jan 2019. 3

[17] S. Liang, L. G. Shapiro, and I. Kemelmacher-Shlizerman. Head reconstruction from internet photos. In *Computer Vision – ECCV 2016*, pages 360–374. Springer International Publishing, 2016. 3

[18] F. Maninchedda, C. Häne, B. Jacquet, A. Delaunoy, and M. Pollefeys. Semantic 3d reconstruction of heads. In *Computer Vision – ECCV 2016*, pages 667–683. Springer International Publishing, 2016. 3

[19] J. Ou, G. Dublon, C.-Y. Cheng, F. Heibeck, K. Willis, and H. Ishii. Cilllia: 3d printed micro-pillar structures for surface texture, actuation and sensing. In *Proceedings of the 2016 CHI Conference on Human Factors in Computing Systems*. ACM, may 2016. 2

[20] S. Paris, W. Chang, O. I. Kozhushnyan, W. Jarosz, W. Matusik, M. Zwicker, and F. Durand. Hair photobooth: geometric and photometric acquisition of real hairstyles. *ACM Transactions on Graphics*, 27(3):1–9, aug 2008. 1

[21] S. Saito, L. Hu, C. Ma, H. Ibayashi, L. Luo, and H. Li. 3d hair synthesis using volumetric variational autoencoders. *ACM Transactions on Graphics*, 37(6):1–12, jan 2019. 2, 3, 8

[22] Y. Shen, C. Zhang, H. Fu, K. Zhou, and Y. Zheng. DeepSketchHair: Deep sketch-based 3d hair modeling. *IEEE Transactions on Visualization and Computer Graphics*, 27(7):3250–3263, jul 2021. 3

[23] J. Sturm, E. Bylow, F. Kahl, and D. Cremers. CopyMe3d: Scanning and printing persons in 3d. In *Lecture Notes in Computer Science*, pages 405–414. Springer Berlin Heidelberg, 2013. 3

[24] M. Teichmann and M. Capps. Surface reconstruction with anisotropic density-scaled alpha shapes. In *Proceedings Visualization '98 (Cat. No.98CB36276)*. IEEE, 1998. 2, 4

[25] J. R. Tena, M. Mahler, T. Beeler, M. Grosse, H. Yeh, and I. Matthews. Fabricating 3d figurines with personalized faces. *IEEE Computer Graphics and Applications*, 33(6):36–46, nov 2013. 3

[26] X. Xu and K. Harada. Automatic surface reconstruction with alpha-shape method. *The Visual Computer*, 19(7-8):431–443, dec 2003. 2, 4, 5

[27] M. Zhang, M. Chai, H. Wu, H. Yang, and K. Zhou. A data-driven approach to four-view image-based hair modeling. *ACM Transactions on Graphics*, 36(4):1–11, jul 2017. 2, 3, 8

[28] H. Zhao. A fast sweeping method for eikonal equations. *Mathematics of Computation*, 74(250):603–627, may 2004. 8

[29] Y. Zhou, L. Hu, J. Xing, W. Chen, H.-W. Kung, X. Tong, and H. Li. HairNet: Single-view hair reconstruction using convolutional neural networks. In *Computer Vision – ECCV 2018*, pages 249–265. Springer International Publishing, 2018. 3

[30] Y. Zhu and R. Bridson. Animating sand as a fluid. *ACM Transactions on Graphics*, 24(3):965–972, jul 2005. 2, 8